Novel Fe loaded activated carbons with tailored properties for As(V) removal: Adsorption study correlated with carbon surface chemistry

Pablo Lodeiro[1], Siu Ming Kwan[2], Jonatan Torres Perez[3], Luisa F. González[4], Claire Gérente[4,*], Yves Andrès[4] and Gordon McKay[2]

[1]*Departamento de Química Física e Enxeñería Química I, Facultad de Ciencias. Universidad de A Coruña, Rúa da Fraga nº 10, 15008, A Coruña, Spain*
[2]*Department of Chemical and Biomolecular Engineering, Hong Kong University of Science and Technology, Clear Water Bay, Kowloon, Hong Kong, P.R. China*
[3]*Universidad Autónoma de Ciudad Juárez, ICB, Departamento de Ciencias Químico-Biológicas, Ciudad Juárez, Chihuahua, México*
[4]*L'UNAM Université, Ecole des Mines de Nantes, CNRS, GEPEA, UMR 6144, 4 rue Alfred Kastler, BP 20722, 44307 Nantes cedex 03, France*

[*] Author to whom correspondence should be addressed
Tel: +33-251858285; E-mail: Claire.Gerente@mines-nantes.fr

ABSTRACT

Novel Fe loaded activated carbons have been prepared from sugar beet pulp (BP) agricultural residues by direct steam activation followed by iron impregnation with or without previous oxidation. The corresponding activated carbons were: BP-H_2O, BP-H_2O-Fe, BP-H_2O-H_2O_2-Fe and BP-H_2O-MnO_2-Fe. The textural characterization of these tailored activated carbons was based on nitrogen adsorption/desorption isotherms leading to BET surface area values between 741-821 m^2/g and total porous volumes between 0.58 and 0.79 cm^3/g. Elemental analysis and ash content showed that carbon content reached 78 % for BP-H_2O with 13.6 % of ash and decreased to 50 % in iron-based materials. BP-H_2O and BP-H_2O-Fe revealed a basic nature with pH_{PZC} values of 9.8 and 9 respectively while BP-H_2O-H_2O_2-Fe and BP-H_2O-MnO_2-Fe had acid pH_{PZC} (5.1 and 3.6). Their surface chemistry has been investigated by XPS analysis and by the quantification of the surface chemical moieties based on Boehm's approach. A clear relationship was found between the surface iron content and the strong acidic groups. Arsenic (As(V)) adsorption isotherms were performed and Langmuir, Freundlich, Redlich-Peterson models were used to describe the experimental data by non-linear regression. It was found that Redlich-Peterson isotherm provided the best fit and the Langmuir adsorption capacities confirmed that the iron-based activated carbons were highly attractive for As(V) removal with capacities up to 17 $mg.g^{-1}$. Finally, it has been shown that the surface iron content determined by XPS analysis is very well correlated with Langmuir q_m values (r^2 = 0.982) and with the strong acidic moieties deduced from the Boehm's method.

Keywords: activated carbon, adsorption, arsenic, iron modified carbon, surface characterization

1. INTRODUCTION

Most environmental arsenic problems are the result of mobilization under natural conditions. However, mining activities, combustion of fossil fuels, the use of arsenic pesticides, herbicides or crop desiccants and the use of arsenic additives to livestock feed create additional impacts. Two predominant species found in natural waters are inorganic forms of arsenic namely, arsenate As(V) and arsenite As(III). Their presence depends on the pH and redox conditions of the medium. As(V) which is the thermodynamically stable form, is found in oxic surface waters, rivers and lakes [1]. Furthermore, arsenate possesses three pKa values (2.3, 6.8 and 11.6): therefore in most of natural waters, As(V) exists mainly in the $H_2AsO_4^-$ or $HAsO_4^{2-}$ forms. Arsenic in natural waters is a serious worldwide problem, especially in Bangladesh and China [2-4]. Long term drinking water exposure causes skin, lung, bladder and kidney cancer as well as pigmentation changes, skin thickening, neurological disorders, muscular weakness, loss of appetite and nausea [5, 6]. Because of this, World Health Organization (WHO), European Union (EU) and US Environmental Protection Agency (USEPA) set the maximum permissible limits for arsenic in drinking water as 10 $\mu g \cdot L^{-1}$. To achieve this, the only possible way is to remove arsenic from water. There is a large amount of literature related to arsenic removal technologies. Mohan and Pittman [7] have published an in depth review on the topic that includes oxidation/precipitation, coagulation/electrocoagulation/co-precipitation, adsorption, ion exchange and membrane techniques. Adsorption has the advantage of being a relatively well-known process when classical sorbents, like activated carbons or iron oxides are used. The problem is that their price is frequently too high regarding their efficiencies. Sorption on raw biomass (biosorption)

or on carbonaceous materials (non porous chars) has also been considered, but the obtained capacities are mostly lower than those achieved with activated sorbents [8]. Therefore, activated carbons produced from agricultural residues or biowastes have been extensively studied. Moreover, iron impregnation at the sorbent surface seems to be a relevant modification to increase the adsorption capacities. Table 1 reports recent data about the removal of arsenic by activated carbons produced from agricultural residues and by commercial ones modified by iron impregnation. Classically, chemical activations use either strong acid, metal salt or other basic agents while physical activation is conducted under steam or CO_2 gas, which is more environmental friendly. The capacities are very variable and globally ranged between 80 and 3000 $\mu g \cdot g^{-1}$. In the third part of this table, numerous iron impregnations are proposed based on commercial materials. Depending on the procedure, capacities range between 20 $\mu g \cdot g^{-1}$ to 20 $mg.g^{-1}$.

In a previous study, activated carbons have been synthesized by direct steam activation from a local precursor [26]. Sugar beet pulp is a residue of the sugar refining industry in France, cheap (100 US$ per metric tonne) and abundant with 14 million tons produced every year in Western Europe, and containing 72.5 % of polysaccharides [27]. The aims of this work are firstly, to prepare and characterize novel Fe-loaded activated carbons with special attention to their surfaces properties and secondly, to study As(V) adsorption. In the first step, original different chemical modifications of these sugar beet based carbons are performed and then their properties, particularly the surface chemistry are investigated. In the second step, arsenic adsorption studies are carried out using contact time experiments and adsorption isotherms. The Langmuir, Freundlich and Redlich-Peterson models are used to describe the

experimental data and their parameters are obtained based on non-linear regression analysis. Relationships between the surface properties and the arsenic removal capacities are also developed.

2. EXPERIMENTAL

2.1. Novel activated carbon production and modification

Sugar beet pulp was obtained from Lyven (Cagny, France) and converted to activated carbons by the following procedure. 150 g raw residues were introduced into a quartz rotary furnace (HTR 11/150, Carbolite) under an inert environment (0.5 L/min of N_2) during the entire process. The furnace was heated up to 857 ºC using a temperature ramp of 10 ºC/min. At 857 °C, the activating gas (steam) was introduced at 0.7 $mL.min^{-1}$ for 80 min. The furnace was finally cooled down to room temperature under a nitrogen atmosphere. These conditions have been optimized based on previous studies [26, 28]. The obtained activated carbon (BP-H_2O) was repeatedly washed in deionised water, dried at 105 ºC and sieved between 0.25 to 0.5 mm. BP-H_2O was then chemically modified in order to impregnate it with iron and to change its structural characteristics. Three different procedures were followed.

Protocol I – Direct iron impregnation without prior oxidation. This protocol was adapted from Haque et al. [29]: 1 g BP-H_2O was mixed with 0.1 M ferric chloride hexahydrate ($FeCl_3.6H_2O$) solution for 24 hours at room temperature with constant agitation at 200 rpm.

Protocol II – Oxidation by hydrogen peroxide (H_2O_2) and then iron impregnation. The protocol was adopted from Muñiz et al. [19] and Haque et al. [29]: 1 g BP-H_2O was mixed with 100 ml 2 M H_2O_2 solution by successive additions at room temperature with constant

agitation at 200 rpm. The oxidized carbon was then placed in 100 ml 0.05 M $FeCl_3.6H_2O$ solution and after 3 days the solution was evaporated at 80 - 90 ºC for 1.5 h.

Protocol III – Oxidation by potassium permanganate ($KMnO_4$) and then iron impregnation. The protocol was adopted from Hristovski et al. [30]: 10 g BP-H_2O were mixed with 150 ml of 0.1 M $KMnO_4$ for 1 hour with constant agitation at 200 rpm. The suspension was filtered and rinsed with deionised water until the filtrate was colorless. Iron impregnation was performed by mixing 1 g oxidized BP-H_2O with 100 ml 0.2 M iron(II) sulfate heptahydrate ($FeSO_4.7H_2O$) for 24 hours at room temperature with constant agitation at 150 rpm.

In all cases, the iron impregnated carbons were successively washed with deionised water until a constant pH was achieved and dried at 105 ºC. They were denoted as BP-H_2O-Fe, BP-H_2O-H_2O_2-Fe and BP-H_2O-MnO_2-Fe respectively.

2.2. Adsorbents characterization and surface analysis

The nitrogen adsorption isotherms, elemental analysis, ash content and pH_{PZC} were performed following the methodologies described previously [26]. The total iron content was determined from an acidic dissolution in aqua regia for 7 days at room temperature and by measurement of the iron concentration in solution by flame atomic absorption spectrometry (Analyst 200, Perkin Elmer). Regarding the surface analysis, two methods were adopted: XPS analysis and the quantification of surface moieties by Boehm's method. XPS analysis (Physical Electronics PHI 5600) provided the elemental surface composition up to 10 nm depth by using a monochromatic Al X-ray source (1486.6 eV) at 350 W, 14 kV, and 25 mA at a vacuum of 1×10^{-8} Torr. Both regular and high-resolution scans were conducted. The

atomic oxidation states can also be analyzed by comparing the measured binding energy with standard samples given in the corresponding handbook [31]. The chemical groups present on the activated carbon surface were investigated through potentiometric titrations (TIM 900 Radiometer) based on the Boehm approach [32]. This is the most reliable method to determine the type and the amount of functional groups in activated carbons [33-36]. The use of basic solutions (0.1 M) with different strengths allowed the identification of diverse acidities. $NaHCO_3$ neutralized the strongest functionalities i.e. the carboxylic groups. Na_2CO_3 also reacted with weak acid sites (weak carboxylic, lactonic groups). NaOH neutralized all the cited groups and the phenolic ones. And HNO_3 (0.1 M) was used for the neutralization of the total basic moieties. The carbon dose (10 g/L) and the contact time (168 h) were optimized and the basic solutions were always saturated with N_2 gas for at least 10 minutes. After filtration, the filtrates were placed in sealed potentiometric cells under a nitrogen atmosphere and titrated with 0.1M standard solutions of HNO_3 or NaOH (Normadose Prolabo, Standard solution). Between each standard solution addition, the equilibrium was considered to be reached when the drift readings were less than 0.5 $mV \cdot s^{-1}$. Moreover, blank control solutions, without activated carbon, were prepared and analysed in the same way. The amount of functional groups was calculated from the difference in the volumes at the equivalence point between control and sample solutions. Two methodologies were used to determine the equivalent points: the derivation of titrations curves (dE/dV) and Gran's graphical method [37] when the detection of equivalent volume was delicate (Figure 1). This technique assumed that added increments of mineral acid linearly increased or decreased proton or hydroxyl concentrations, respectively. In the case of an acid titration by a strong

base (Figure 1a) and since the glass electrode exhibits a Nernstian response, Eq. (1) and (2) can be obtained, before and after the equivalence point respectively:

$$E = E^0 + s\log\frac{(c_a v_0 - c_b v_{ad})}{(v_0 + v_{ad})} \quad (1)$$

$$E = E^0 + s\log\frac{K_w(v_0 + v_{ad})}{(c_a v_0 - c_b v_{ad})} \quad (2)$$

where E is the potential measured by the electrode, E^0 the standard potential, s denoted the Nernstian slope (59.16 mV at 25 ºC), K_W is the ionic product of water, v_0 and v_{ad} are the initial and added volume, respectively; c_a and c_b represents the initial concentrations of acid and base, respectively. At the equivalence point, it can be written:

$$v_0 \times c_a = v_{eq} \times c_b \quad (3)$$

Substitution of $c_a \cdot v_0$ by $c_b \cdot v_{eq}$ in Eq. 1 and subsequent rearrangement leads to the following Gran function:

$$\psi = (v_0 + v_{ad})10^{pH} = c_b(v_{eq} - v_{ad}) \quad (4)$$

A plot ψ vs. v_{ad} provides a straight line that intercepts the x-axis at $v_{ad} = v_{eq}$ (Figure 1b). Following the analogous procedure for Eq. 2, the Gran function for basic media was obtained:

$$\psi' = (v_0 + v_{ad})10^{-pH} = \frac{c_b}{K_w}(v_{ad} - v_{eq}) \quad (5)$$

In the same way, a plot of ψ´vs. v_{ad} leads to a second straight line, which intercepted the x-axis at the same point as the function ψ (Figure 1b). In order to give the best precision to the equivalence detection, all the equivalent points of potentiometric curves were systematically checked with the Gran's method. Average values of functional groups concentration were obtained from two or three different experiments made at least in

duplicate. Typical errors were found to be between 2 and 10 % of the reported means.

2.4. Arsenic adsorption experiments and modeling

The effect of contact time on As(V) removal was studied at room temperature by putting 0.05 g each of BP-H_2O and BP-H_2O-Fe adsorbent into 100 ml of arsenic solution with initial As(V) concentrations of 100, 500, and 1000 $\mu g \cdot L^{-1}$. The solutions were agitated at 300 rpm in polyethylene bottles. Batch experiments were also conducted in the same conditions with 0.05 g adsorbent into 100 ml of arsenic solutions. Initial pH (before introduction of AC) and final pH were recorded. The arsenic concentration in solutions was measured by an atomic absorption spectrometer equipped with a graphite furnace (PerkinElmer® 600 AAnalyst) leading to a detection limit of 2 $\mu g.L^{-1}$.

The equilibrium data were analyzed in accordance with the Langmuir, Freundlich and Redlich-Peterson isotherm models. They are usually applied for the single component adsorption. The Langmuir equation is:

$$q_e = \frac{q_m b_L C_e}{1 + b_L C_e} \tag{6}$$

where q_m ($\mu g \cdot g^{-1}$ of dry weight) is the maximum adsorption capacity corresponding to complete monolayer coverage, C_e ($\mu g \cdot L^{-1}$) is the equilibrium solute concentration, and b_L ($L \cdot \mu g^{-1}$) is the equilibrium constant related to the energy of sorption. The Freundlich isotherm is:

$$q_e = K_f C_e^n \tag{7}$$

where K_f ($(\mu g \cdot g^{-1})/(\mu g \cdot L^{-1})^{1/n}$), and n are the Freundlich isotherm constants related to the adsorption capacity and the degree of favorability of adsorption, respectively. Finally, the

Redlich-Peterson equation is:

$$q_e = \frac{K_R C_e}{1 + b_R C_e^{\gamma}} \tag{8}$$

where K_R, b_R and γ are the isotherm constants. K_R ($L \cdot g^{-1}$) is the solute adsorptivity, b_R ($L \cdot \mu g^{-1}$) related to adsorption energy and γ is the heterogeneity constant ($0<\gamma<1$).

The Langmuir, Freundlich and Redlich-Peterson parameters were obtained by plotting nonlinear least-squares regression analysis (Kaleida Graph®). To examine the accuracy of the fitting of the experimental data by the aforementioned isotherms, the coefficient of determination, r^2, was computed and is given as follows:

$$r^2 = \frac{\sum \left(q_{e,\exp} - \bar{q}_{e,\exp}\right)^2 - \sum \left(q_{e,\exp} - q_{e,cal}\right)^2}{\sum \left(q_{e,\exp} - \bar{q}_{e,\exp}\right)^2} \tag{9}$$

where $q_{e,cal}$ is the equilibrium capacity obtained from the isotherm model, $q_{e,exp}$ is the equilibrium capacity obtained from experiment and $\bar{q}_{e,\exp}$ is the average value of $q_{e,exp}$.

3. RESULTS AND DISCUSSION

3.1. Characterization of adsorbents

The four activated carbons (BP-H_2O, BP-H_2O-Fe, BP-H_2O-H_2O_2-Fe and BP-H_2O-MnO_2-Fe) produced by direct steam activation from sugar beet pulp and modified by iron impregnation have been characterized. Their main properties are summarized in Table 2 including the global and the surface characterization. BP-H_2O has a surface area value of 821 $m^2 \cdot g^{-1}$, which is quite good compared to other data obtained from direct steam activation of agricultural by-products. At 800 ºC, for an activation of 1h with 120 $mL \cdot min^{-1}$ of steam flow rate, Savova et al. found BET surface areas ranging between 500 and 1200 $m^{2} \cdot g^{-1}$

depending on the precursor [38]. For apricot stones, Gergova and Eser reported surface areas ranging between 380 and 930 $m^2 \cdot g^{-1}$ as a function of the activation temperature [39]. When iron impregnation is used, no great differences were found with respect of the original area values. It means that whatever the chemical treatment, the surface is not homogeneously coated by iron. This is also confirmed by the SEM images and EDX spectra (data not shown in here) where specific spots of iron have been observed. In terms of porous volumes, BP-H_2O and BP-H_2O-Fe have equal micro and mesoporous volumes close to 0.35 $cm^3 \cdot g^{-1}$ and 0.32 $cm^3 \cdot g^{-1}$ respectively. Compared with the literature data, similar pore volumes can be found again according to the precursors or the differences in the activation conditions [36, 38-40]. The high carbon content (> 68 %) and good BET surface area (> 762 $m^2 \cdot g^{-1}$) found in BP-H_2O, BP-H_2O-Fe and BP-H_2O-H_2O_2-Fe and to a lesser extent in BP-H_2O-MnO_2-Fe prove that these carbonaceous materials are really active carbons. Oxygen is another interesting element since its content is generally related to the acid-base character of the material. The increase of the oxygen content indicates a more acidic behaviour [36]. A partial oxidation of the carbon is possible when iron is impregnated, as the metallic solution is acidic. This gives the oxygen content increased from 7 % (BP-H_2O) to 16 % (BP-H_2O-Fe). After a stronger oxidation by H_2O_2 or $KMnO_4$, the mesoporous volumes increased up to 0.49 $cm^3 \cdot g^{-1}$ in BP-H_2O-H_2O_2-Fe and BP-H_2O-MnO_2-Fe. The oxidation partially modifies the surface structure such as the macroporous network and certainly widens the mesopores. As far as oxygen is considered, 22% has been detected in BP-H_2O-MnO_2-Fe and 9% in BP-H_2O-H_2O_2-Fe is surprisingly low. A trace amount of total iron (0.1 %) has been found in BP-H_2O and this content depends on the treatment protocol: 4.8 % of iron was observed in

BP-H_2O-Fe while it can reach up to 20 % for BP-H_2O-MnO_2-Fe. In this case, it also produces a diminution in the carbon content and in the pH_{pzc} value. This is in agreement with the values presented in literature for commercial activated carbons [18]. Ash content in BP-H_2O (14 %) is relatively high for an active carbon, but it is probably due to the presence of calcium (1.1 %) in the raw structure of the sugar beet pulp [27]. Regarding the pH_{pzc} BP-H_2O and BP-H_2O-Fe exhibit a basic nature probably due to the π-electrons of the graphene layers and some surface oxygenated functions like chromenol, pyrones and quinones [20]. This is quite an accepted feature for carbons activated with steam. After an oxidative treatment and an iron impregnation, the pH_{pzc} values decrease to 5.1 for BP-H_2O-H_2O_2-Fe and 3.6 for BP-H_2O-MnO_2-Fe. The oxidation step generated more acidic oxygenated functional groups such as carboxyl, anhydrides, hydroxyls, lactones and lactol groups at the edge of the graphene layers as well as the surface [20]. These results are well correlated with Boehm titrations presented later.

As far as the surface characterization is concerned, the iron content (Fe_{XPS} in %) is among the most interesting results obtained with the XPS analysis (Table 2). Only 1 % is detected at the surface of BP-H_2O but a strong increase following to the iron impregnation is observed and reached 5, 10 and 32% in BP-H_2O-Fe, BP-H_2O-H_2O_2-Fe and BP-H_2O-MnO_2-Fe respectively. These surface concentrations are usually higher than the total iron content since iron has been added in some specific sites seen in SEM pictures. Moreover, the iron chemical state for the iron-impregnated samples is obtained from NIST X-ray photoelectron spectroscopy database by using the binding energy of Fe2p 3/2 peaks (figure not shown). BP-H_2O-Fe also presents a peak with a binding energy around 712.3 eV ascribed

to $Ca_3Fe_2(SiO_4)_3$ or FeS probably due to presence of calcium in the raw sugar beet pulp [27] and which is certainly concentrated during the pyrolysis and activation process. Regarding BP-H_2O-H_2O_2-Fe and BP-H_2O-MnO_2-Fe, the binding energy of the Fe peak was 711.6 eV, which corresponds to Fe_2O_3 species. To strengthen the quantitative knowledge on the carbon surface, further work comprised to titrating the chemical moieties with the Boehm's approach (Table 2). The total basic functions are very high in BP-H_2O (2.16 meq.g^{-1}) and decrease gradually in BP-H_2O-Fe (1.59 meq.g^{-1}), then in BP-H_2O-H_2O_2-Fe (0.6 meq.g^{-1}) and in BP-H_2O-MnO_2-Fe (0.23 meq.g^{-1}) while the total acidic moieties increase from 0.52 to 1.75 meq.g^{-1} respectively. These results are completely in agreement with the pH_{PZC} values and a high linear correlation (r^2 = 0.962) has be found in the case of the total basic groups (Figure 2). The surface of BP-H_2O presents few acidic moieties consistent with the high value of pH_{PZC} (9.8), including weak or very weak acidity (0.24 and 0.28 meq.g^{-1} respectively) and no strong acidity at all. These balances change with the iron impregnation leading to a great increase of very strong acidic functions (0.77 meq.g^{-1}) and in a lesser extent the very weak ones (0.61 meq.g^{-1}) in BP-H_2O-MnO_2-Fe. In Figure 3, the plot of the strong acidic groups versus the surface iron content (Fe_{XPS}) displays perfect linearity (r^2 = 0.995) for the 4 materials. These correlations between characterisation parameters are quite interesting and could be correlated with adsorption capacities in the next section.

3.2. Arsenic batch adsorption

3.2.1 Contact time experiment

Kinetic decay curves of BP-H_2O and BP-H_2O-Fe have been plotted in Figure 4 for

different initial As(V) concentrations. Open symbols correspond to BP-H_2O and filled symbols correspond to BP-H_2O-Fe. Although some points seem to be close to 0 $\mu g \cdot L^{-1}$ (for BP-H_2O-Fe, C_0 = 100 $\mu g \cdot L^{-1}$), it has been verified that all the data are higher than the detection limit determined by GF-AAS for As(V) measurement (2 $\mu g \cdot L^{-1}$). There is a low adsorption of As(V) on BP-H_2O and the adsorption capacities are greatly improved for BP-H_2O-Fe. The equilibrium time is different for the two materials. 24 hours (1 day) was enough for BP-H_2O to reach equilibrium while BP-H_2O-Fe needed 96 hours (4 days). Because of the great difference in equilibrium time required for different adsorbents, the contact time has been fixed at 120 hours (5 days) for all the adsorption experiments to ensure enough time to reach equilibrium.

3.2.2 Adsorption isotherms

The As(V) batch adsorption isotherms have been performed for various initial concentrations with the four different adsorbents (Figure 5). There is such a huge difference between the capacities of BP-H_2O and BP-H_2O-MnO_2-Fe that a change of scale was necessary. Several reasons may explain these differences. As far as the speciation is concerned, the pH is the most important parameter in these adsorption reactions. With long equilibrium time, the final pH is considered as the working pH since it has not been adjusted. The measured values were the followings: 9.1 to 9.4 for BP-H_2O, 8.5 to 9.1 for BP-H_2O-Fe, 4.9 to 6.1 for BP-H_2O-H_2O_2-Fe and 4.2 to 5.6 for BP-H_2O-MnO_2-Fe. With a pH_{PZC} of 9.8 (Table 2), BP-H_2O probably presents a positively charged surface due to the protonation of the chemical moieties. With the same analysis, BP-H_2O-Fe is more neutral, BP-H_2O-H_2O_2-Fe is balanced between neutrality and negative charge and BP-H_2O-MnO_2-Fe is quite negative.

Between pH 4 to 10, the predominant species of arsenate are therefore $H_2AsO_4^-$ and $HAsO_4^{2-}$. Then a favourable electrostatic attraction between the $HAsO_4^{2-}$ anionic species and the global positive charge of the surface can explain the adsorption onto BP-H_2O. For the other adsorbents, there is competition between electrostatic attraction/repulsion and the affinity to iron discussed later. Three adsorption models (Langmuir, Freundlich and Redlich-Peterson) have been used to describe the experimental isotherms (Figure 6) by non-linear regression fit, and their parameters are listed in Table 3. The Redlich-Peterson isotherm provides the best fit for all adsorbents; nevertheless, it must be taken into account that this model uses three adjustable parameters, instead of the two used in Langmuir or Freundlich equations. From the Langmuir equation, the q_m values of BP-H_2O, BP-H_2O-Fe, BP-H_2O-H_2O_2-Fe and BP-H_2O-MnO_2-Fe are 0.69 mg·g^{-1}, 2.94 mg·g^{-1}, 3.25 mg·g^{-1} and 16.8 mg·g^{-1} respectively. A comparison with the literature values (Table 1) shows that BP-H_2O displays a maximum capacity lower than those obtained by Chuang et al. [13]. On the other hand, the iron impregnation leads to capacities close to those reported with commercial activated carbons. Very recently, Nieto-Delgado and Rangel-Mendez [41] published similar work with chemically activated agave bagasse based activated carbons. Their Langmuir parameters are not available but if equilibrium capacities are considered, adsorption isotherms show capacities close to 1 mg.g^{-1} (at an equilibrium concentration of 2 mg.L^{-1}) compared to 2.5 to 17 mg.g^{-1} with BP-H_2O-Fe, BP-H_2O-H_2O_2-Fe and BP-H_2O-MnO_2-Fe (at the same equilibrium concentration). Expressed in terms of iron loading, the adsorption capacities of BP-H_2O-H_2O_2-Fe and BP-H_2O-MnO_2-Fe are 108 and 84 mg As(V)/g Fe, respectively. They are similar to those obtained by Nieto-Delgado and Rangel-Mendez [41]. In order to link

together the surface properties and the adsorption capacities, very good relationships have been found between the q_m values of Langmuir and the surface iron content (Fe_{XPS}) in Figure 7 (r^2=0.982), or between the q_m values of Langmuir and the quantity of strong acid groups (r^2 = 0.982, data not shown). It is then obvious that the presence of iron and strong acidic moieties at the surface coupled with high mesoporous volumes and BET surface areas greatly increase the arsenate adsorption.

4. CONCLUSION

Novel activated carbons based on sugar beet pulp have been synthesized by direct steam activation followed by an iron impregnation. Several characterisations have been performed including the textural parameters essential to the adsorption process as well as the chemical composition focused particularly on the surface. They display tailored properties particularly attractive for arsenate removal leading to adsorption capacities up to 17 $mg.g^{-1}$. These performances are mainly due to the iron content and the strong acidic moieties at the surface with added high porosity.

ACKNOWLEDGEMENT

The authors are grateful to the support of the Ministère des Affaires étrangères et européennes (MAEE) and the Ministère de l'Enseignement supérieur et de la Recherche (MESR) of France. P. Lodeiro gratefully acknowledges financial support through Ángeles Alvariño projects AA 10.02.56B.44.0 and 10.02.561B.480.0 (from Xunta de Galicia, Spain) both

co-funded by 80 % with European Social Funds. S.M. Kwan thanks Hong Kong University of Science and Technology, the General Consulate of France in Hong Kong and Ecole des Mines de Nantes for the post-doctorate fellowship. J. Torres Perez is grateful to the Council of Science and Technology of Mexico (CONACYT) and to the Public Education Secretary (SEP) for his PhD grant. Luisa F. González acknowledges financial support of Civil and Environmental Engineering Department and Engineering Faculty of Universidad de los Andes (Bogotá, Colombia).

References

[1] P.L. Smedley, D.G. Kinniburgh, A review of the source, behaviour and distribution of arsenic in natural waters. Appl. Geochem. 17 (2002) 517-568.

[2] B.K. Mandal, K.T. Suzuki, Arsenic round the world: a review. Talanta. 58 (2002) 201–235.

[3] M.M. Karim, Arsenic in groundwater and health problems in Bangladesh. Water Res. 34 (2000) 304-310.

[4] G. Sun, Arsenic contamination and arsenicosis in China. Toxicol. Appl. Pharmacol. 198 (2004) 268–271.

[5] C.K. Jain, I. Ali, Arsenic: Occurrence, toxicity and speciation techniques. Water Res. 34 (2000) 4304-4312.

[6] WHO, Arsenic, in Environmental Health Criteria 18. 1981, World Health Organization, Geneva.

[7] D. Mohan, C.U. Pittman, Arsenic removal from water/wastewater using adsorbents - A critical review. J. Hazard. Mater. 142 (2007) 1-53.

[8] D.S. Tavares, C.B. Lopes, J.P. Coelho, M.E. Sánchez, A.I. Garcia, A.C. Duarte, M. Otero, E. Pereira, Removal of arsenic from aqueous solutions by sorption onto sewage sludge based sorbent. Wat. Air and Soil Pol. 223 (2012) 2311-2321.

[9] T. Budinova, N. Petrov, M. Razvigorova, J. Parra, P. Galiatsatou, Removal of arsenic(III) from aqueous solution by activated carbons prepared from solvent extracted olive pulp and olive stones. Ind. Eng. Chem. Res. 45(2006) 1896-1901.

[10] P. Mondal, C.B. Majumder, B. Mohanty, Removal of trivalent arsenic (As(III)) from contaminated water by calcium chloride ($CaCl_2$)-impregnated rice husk carbon. Ind. Eng. Chem. Res. 46 (2007) 2550-2557.

[11] M.I. Jahan, M.A. Motin, M. Moniuzzaman, M. Asadullah, Arsenic removal from water using activated carbon obtained from chemical activation of jute stick. Indian J. Chem. Technol. 15 (2008) 413-416.

[12] D. Kalderis, D. Koutoulakis, P. Paraskeva, E. Diamadopoulos, E. Otal, J. Oliverares del Valle, C. Fernández-Pereira, Adsorption of polluting substances on activated carbons prepared from rice husk and sugarcane bagasse. Chem. Eng. J. 144 (2008) 42-50.

[13] C.L. Chuang, M. Fan, M. Xu, R.C. Brown, S. Sung, B. Saha, C.P. Huang, Adsorption of arsenic(V) by activated carbon prepared from oat hulls. Chemosphere. 61 (2005) 478-483.

[14] T. Budinova, D. Savova, B. Tsyntsarski, C.O. Ania, B. Cabai, J.B. Parra, N. Petrov, Biomass waste-derived activated carbon for the removal of arsenic and manganese ions from aqueous solutions. Appl. Surf. Sci. 255 (2009) 4650-4657.

[15] B.E. Reed, R. Vaughan, and L.Q. Jiang, As(III), As(V), Hg, and Pb removal by Fe-oxide impregnated activated carbon. J. Environ. Eng. 126 (2000) 869-873.

[16] P. Mondal, C.B. Majumder, B. Mohanty, Effects of adsorbent dose, its particle size and initial arsenic concentration on the removal of arsenic, iron and manganese from simulated ground water by Fe^{3+} impregnated activated carbon. J. Hazard. Mater. 150 (2008) 695-702.

[17] Z.M. Gu, J. Fang, B.L. Deng, Preparation and evaluation of GAC-based iron-containing adsorbents for arsenic removal. Environ. Sci. Technol. 39 (2005) 3833-3843.

[18] V. Fierro, G. Muñiz, G. Gonzalez-Sánchez, M.L. Ballinas, A. Celzard, Arsenic removal by iron-doped activated carbons prepared by ferric chloride forced hydrolysis. J. Hazard. Mater. 168 (2009) 430-437.

[19] G. Muñiz, V. Fierro, A. Celzard, G. Furdin, G. Gonzalez-Sánchez, M.L. Ballinas, Synthesis, characterization and performance in arsenic removal of iron-doped activated carbons prepared by impregnation with Fe(III) and Fe(II). J. Hazard. Mater. 165 (2009) 893-902.

[20] M. Jang, W. Chen, F.S. Cannon, Preloading hydrous ferric oxide into granular activated carbon for arsenic removal, Environ. Sci. Technol., 42 (2008) 3369-3374.

[21] H. Zhu, Y.F. Jia, X. Wu, H. Wang, Removal of arsenic from water by supported nano zero-valent iron on activated carbon. J. Hazard. Mater. 172 (2009) 1591-1596.

[22] J.M. Zhuang, E. Hobenshield, T. Walsh, Arsenate sorption by hydrous ferric oxide incorporated onto granular activated carbon with phenol formaldehyde resins coating. Environ. Technol. 29 (2008) 401-411.

[23] Z.M Gu, B.L. Deng, Use of iron-containing mesoporous carbon (IMC) for arsenic removal from drinking water. Environ. Eng. Sci. 24 (2007) 113-121.

[24] R.L. Vaughan, B.E. Reed, E.H. Smith, Modeling As(V) removal in iron oxide impregnated activated carbon columns. J. Environ. Eng. 133 (2007) 121-124.

[25] E. Deliyanni, T.J. Bandosz, Importance of carbon surface chemistry in development of iron-carbon composite adsorbents for arsenate removal. J. Hazard. Mater. 186 (2011) 667-674.

[26] J. Torres Perez, C. Gerente, Y. Andres, Conversion of agricultural residues into activated carbons for water purification: Application to arsenate removal. J. Environ. Sci. Heal. A. 47 (2012) 1173-1185.

[27] Z. Reddad, C. Gerente, Y. Andres, P. Le Cloirec, Adsorption of several metal ions onto a low-cost biosorbent: kinetic and equilibrium studies, Environ. Sci. Technol. 36 (2002) 2067-2073.

[28] S. Rio, L. Le Coq, C. Faur, D. Lecomte, P. Le Cloirec, Preparation of adsorbents from sewage sludge by steam activation for industrial emission treatment. Process Saf. Environ. Prot. 84 (2006) 258-264.

[29] N. Haque, G. Morrison, I. Cano-Aguilera, J.L. Gardea-Torresdey, Iron-modified light expanded clay aggregates for the removal of arsenic(V) from groundwater. Microchem. J. 88 (2008) 7-13.

[30] K.D. Hristovski, P. Westerhoff, T. Moller, P. Sylvester, Effect of synthesis conditions on nano-iron (hydr)oxide impregnated granulated activated carbon. Chem. Eng. J. 146 (2009) 237-243.

[31] J.F. Moulder, W.F. Stickle, P.E. Sobol, K.D. Bomben, Handbook of X-ray photoelectron spectroscopy : a reference book of standard spectra for identification and interpretation of XPS data, ed. J. Chastain. 1992: Physical Electronics Division, Perkin-Elmer Corporation.

[32] H.P. Boehm, Chemical Identification of Surface Groups, in Advances in Catalysis and Related Subjects, D.D. Eley, H. Pines, and P.B. Weisz, Editors. 1966, Academic Press: New York and London. 179-225.

[33] A. Contescu, M. Vass, C. Contescu, K. Putyera, J.A. Schwarz, Acid buffering capacity of basic carbons revealed by their continuous pH distribution. Carbon. 36 (1998) 247-258.

[34] A. Contescu, C. Contescu, K. Putyera. J.A. Schwarz, Surface acidity of carbons characterized by their continuous pK distribution and Boehm titration. Carbon. 35 (1997) 83-94.

[35] H.P. Boehm, Surface oxides on carbon and their analysis: a critical assessment. Carbon. 40 (2002) 145-149.

[36] T.J. Bandosz, C.O. Ania, Chapter 4 Surface chemistry of activated carbons and its characterization, in Interface Science and Technology, J.B. Teresa, Editor. 2006, Elsevier. 159-229.

[37] G. Gran, Determination of the Equivalent Point in Potentiometric Titrations, Acta Chem. Scand. 4 (1950) 559-577.

[38] D. Savova, E. Apak, E. Ekinci, F. Yardim, N. Petrov, T. Budinova, M. Razvigorova, V. Minkova, Biomass conversion to carbon adsorbents and gas. Biomass Bioenerg. 21 (2001) 133-142.

[39] K. Gergova, S. Eser, Effects of activation method on the pore structure of activated carbons from apricot stones. Carbon, 34 (1996) 879-888.

[40] A.N.A. El-Hendawy, S.E. Samra, and B.S. Girgis, Adsorption characteristics of activated carbons obtained from corncobs. Colloid Surf. A-Physicochem. Eng. Asp. 180 (2001) 209-221.

[41] C. Nieto-Delgado, J.R. Rangel-Mendez, Anchorage of hydro(oxide) nanoparticles onto activated carbon to remove As(V) from water, Wat. Res. 46 (2012) 2973-2982.

Table 1. Maximum adsorption capacities from Langmuir model of arsenic on activated carbons produced from agricultural residues and iron impregnated activated carbons

Precursor	Activation/Modification	Maximum adsorption capacities from Langmuir model (q_m)		Reference
		As(III)	As(V)	
Part I. Chemically activated carbons from agricultural residues				
Olive pulp	K_2CO_3	860 $\mu g \cdot g^{-1}$	---	
Olive stone	K_2CO_3	740 $\mu g \cdot g^{-1}$	---	Budinova et al., [9]
	H_2O/HNO_3	210 $\mu g \cdot g^{-1}$	---	
Rice husk	$CaCl_2$	18.2 $\mu g \cdot g^{-1}$	---	Mondal et al., [10]
Jute stick	H_3PO_4	---	75 $\mu g \cdot g^{-1}$	Jahan et al., [11]
Rice husk	$ZnCl_2/CO_2$	1220 $\mu g \cdot g^{-1}$	---	Kalderis et al., [12]
Part II. Physically activated carbons from agricultural residues				
Oat hulls	H_2O	---	3100 $\mu g \cdot g^{-1}$	Chuang et al., [13]
Olive pulp	H_2O/2h	1390 $\mu g \cdot g^{-1}$	---	Budinova et al., [9]
Bean pods waste	H_2O/1h	1010 $\mu g \cdot g^{-1}$	---	Budinova et al., [14]
Part III. Iron impregnated activated carbons				
Lignite coal	Fe(IIII)	---	4500 $\mu g \cdot g^{-1}$	Reed et al., [15]
Commercial activated carbon	2.5% $FeCl_3$ (pH=12)	---	24 $\mu g \cdot g^{-1}$	Mondal et al., [16]
Commercial activated carbon (Darco)	0.1 M $FeCl_2$	---	6570 $\mu g \cdot g^{-1}$	Gu et al., [17]
Commercial activated carbon	0.05M $FeCl_3$	---	28 $\mu g \cdot g^{-1}$	Fierro et al., [18]
Commercial activated carbon (NC-100)	0.05M $FeCl_3$ + 3M HCl	---	25-30 $\mu g \cdot g^{-1}$	Muñiz et al., [19]
Commercial activated carbon (SuperDarco)	0.5-1 g/ml [$FeNO_3 \cdot 9H_2O$]	---	18000-20000 $\mu g \cdot g^{-1}$	Jang et al., [20]
Coal-derived activated carbon	$FeSO_4$ + $NaBH_4$	18200 $\mu g \cdot g^{-1}$	12000 $\mu g \cdot g^{-1}$	Zhu et al., [21]
Commercial activated carbon	Phenol formaldehyde + FeO	---	85 % of As(V) removal with C_o = 1.74 $mg \cdot L^{-1}$	Zhuang et al., [22]
Mesoporous carbon	Sodium hypochloride + $FeCl_3$	5960 $\mu g \cdot g^{-1}$	5150 $\mu g \cdot g^{-1}$	Gu et al., [23]
Commercial activated carbon	FeO	---	9100 $\mu g \cdot g^{-1}$	Vaughan et al., [24]
Commercial activated carbon	$FeNO_3$ + 70% HNO_3	---	18900 $\mu g \cdot g^{-1}$	Deliyanni et al.,[25]

Table 2. Properties of the prepared adsorbents

		BP-H_2O	BP-H_2O-Fe	BP-H_2O-H_2O_2-Fe	BP-H_2O-MnO_2-Fe
Global characterization					
N_2 adsorption isotherm	S_{BET} ($m^2 \cdot g^{-1}$)	821	762	858	741
	V_{micro} ($cm^3 \cdot g^{-1}$)	0.35	0.32	0.36	0.31
	V_{meso} ($cm^3 \cdot g^{-1}$)	0.36	0.32	0.49	0.47
	V_{total} ($cm^3 \cdot g^{-1}$)	0.64	0.58	0.79	0.69
Elemental analysis	C_{TOT} (%)	78	68	77	50
	O_{TOT} (%)	7.0	16	9.0	22
Fe_{TOT} (%)		0.1	4.8	3.0	20
Ash (%)		13.6	13.9	7.6	33.2
pH_{pzc}		9.8	9.0	5.1	3.6
Surface characterization					
Fe_{XPS} (%)		1	5	10	32
Total basic moieties ($meq \cdot g^{-1}$)		2.16	1.59	0.60	0.23
Total acidic moieties ($meq \cdot g^{-1}$)		0.52	0.70	1.15	1.75
Very weak acidic moieties ($meq \cdot g^{-1}$)		0.28	0.38	0.59	0.61
Weak acidic moieties ($meq \cdot g^{-1}$)		0.24	0.19	0.30	0.37
Strong acidic moieties ($meq \cdot g^{-1}$)		0	0.12	0.26	0.77

Table 3. Isotherm parameters obtained by non-linear regression fit for the prepared adsorbents

Sample	Langmuir isotherm			Freundlich isotherm			Redlich-Peterson			
	q_m (μg/g)	b_L (L/μg)	r^2	K_f ((μg/g)/(μg/L)$^{1/n}$)	n	r^2	K_R (L/g)	b_R (L/μg)	γ	r^2
BP-H_2O	691	0.00066	0.9556	11.5	0.457	0.9862	86.5	7.422	0.545	0.9862
BP-H_2O-Fe	2936	0.00312	0.9639	205	0.331	0.9901	60	0.192	0.723	0.9951
BP-H_2O-H_2O_2-Fe	3246	0.00421	0.9448	395	0.261	0.9991	451	1.070	0.747	0.9993
BP-H_2O-MnO_2-Fe	16844	0.07900	0.9833	6794	0.136	0.9364	1819	0.142	0.958	0.9885

FIGURE CAPTIONS

FIGURE 1. (a) Titration of HNO_3 with NaOH after contact with BP-H_2O (open circles) and the corresponding derivate (continuous line). (b) Gran representation for the titration showed in (a). Acid regression (squares) and basic regression (triangles) with the corresponding linear fits, ψ and ψ'.

FIGURE 2. Relation between the concentrations of acid (squares) or basic (circles) moieties and the corresponding pH_{pzc} values for sugar beet pulp derived carbons.

FIGURE 3. Relation between the strong acidic moieties and the corresponding iron content (Fe % from XPS analysis).

FIGURE 4. Kinetic decay curves for the removal of As(V) by BP-H_2O (open symbols) and BP-H_2O-Fe (filled symbols) at different initial concentrations: 100 μg/L (diamonds), 500 μg/L (squares) and 1000 μg/L (triangles)

FIGURE 5. Experimental adsorption isotherms of arsenate onto BP-H_2O (diamonds), BP-H_2O-Fe (squares), BP-H_2O-H_2O_2-Fe (triangles) and BP-H_2O-MnO_2-Fe (circles).

FIGURE 6. Adsorption isotherm for (a) BP-H_2O, (b) BP-H_2O-Fe, (c) BP-H_2O-H_2O_2-Fe and (d) BP-H_2O-MnO_2-Fe. The lines correspond to Langmuir (discontinuous), Freundlich (continuous) and Redlich-Peterson (dotted with starts) models.

FIGURE 7. Relation between q_m and the corresponding iron content (Fe % from XPS analysis).

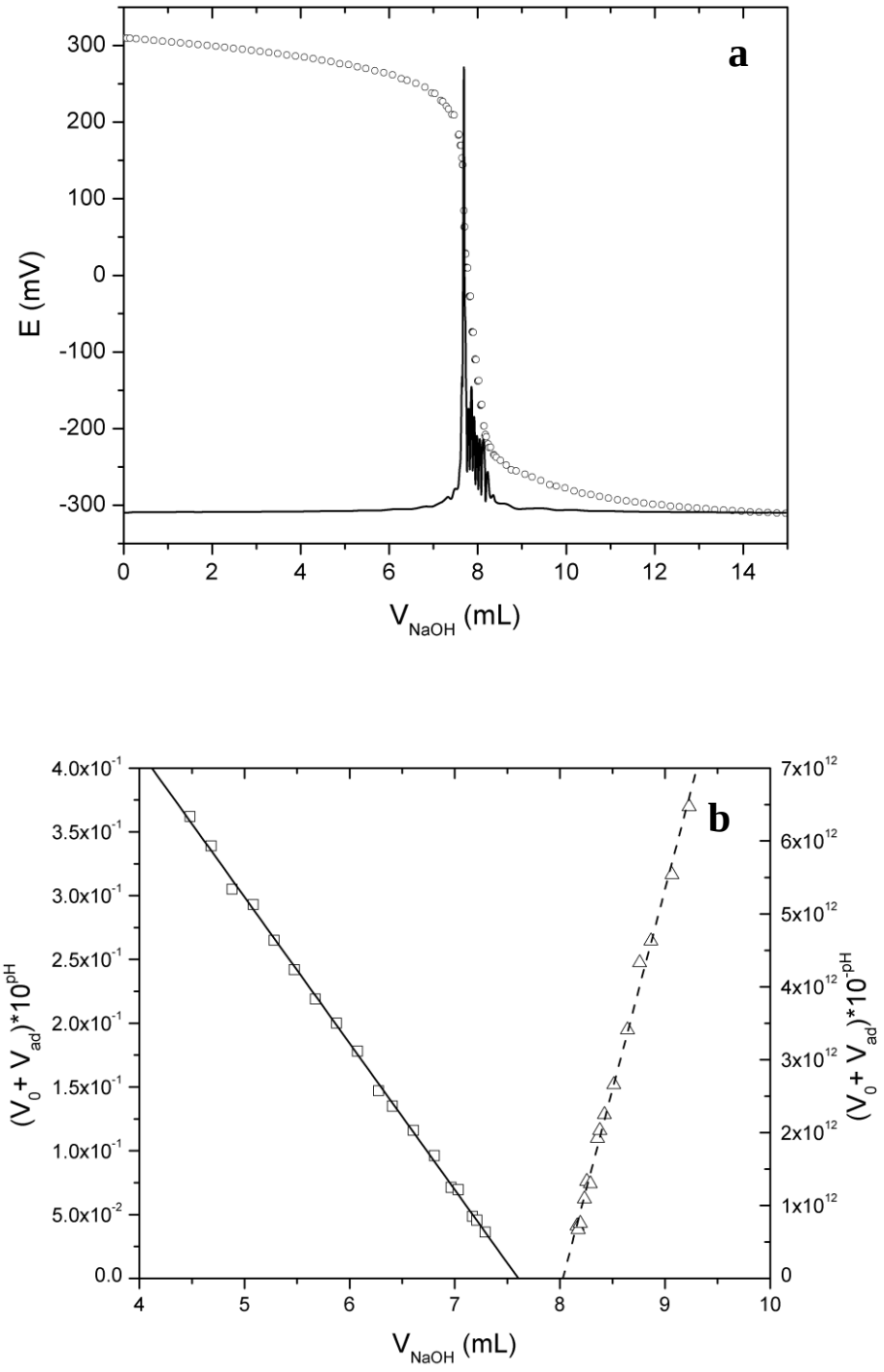

FIGURE 1. (a) Titration of HNO_3 with NaOH after contact with BP-H_2O (open circles) and the corresponding derivate (continuous line). (b) Gran representation for the titration showed in (a). Acid regression (squares) and basic regression (triangles) with the corresponding linear fits, ψ and ψ'.

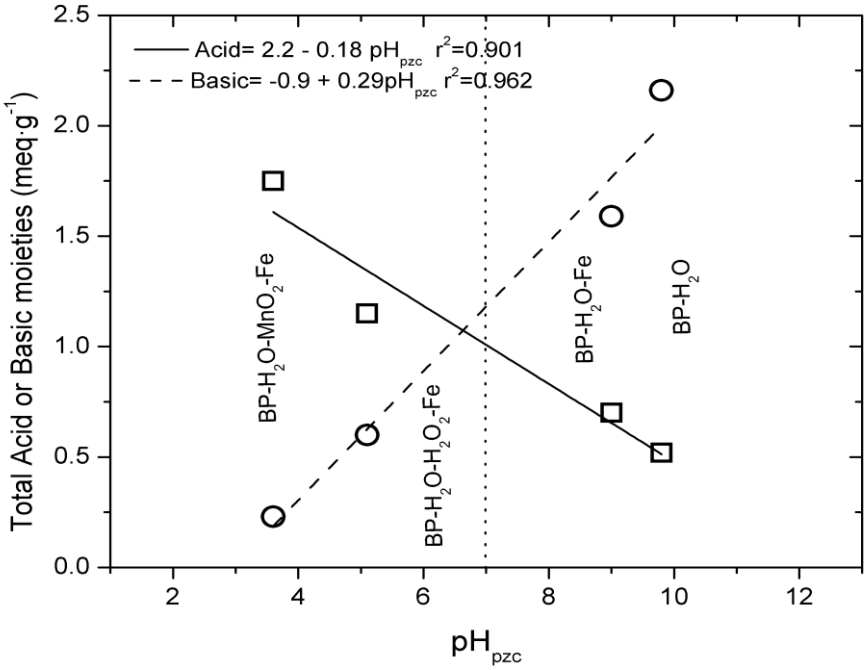

FIGURE 2. Relation between the concentrations of acid (squares) or basic (circles) moieties and the corresponding pH_{pzc} values for sugar beet pulp derived carbons.

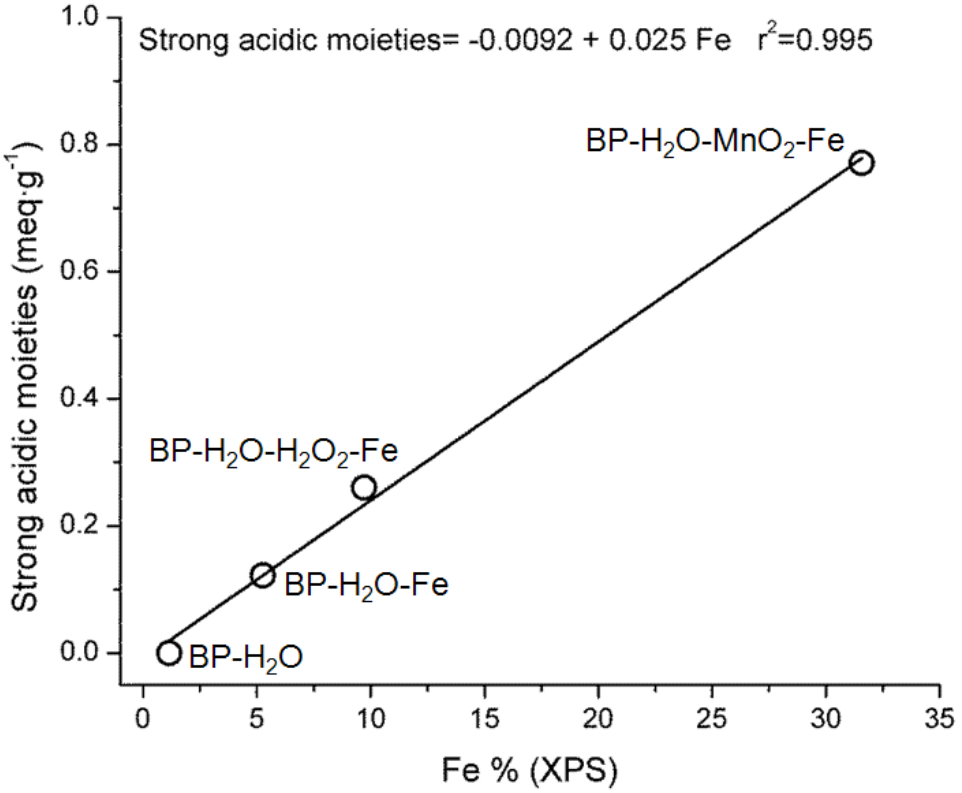

FIGURE 3. Relation between the strong acidic moieties and the corresponding iron content (Fe % from XPS analysis).

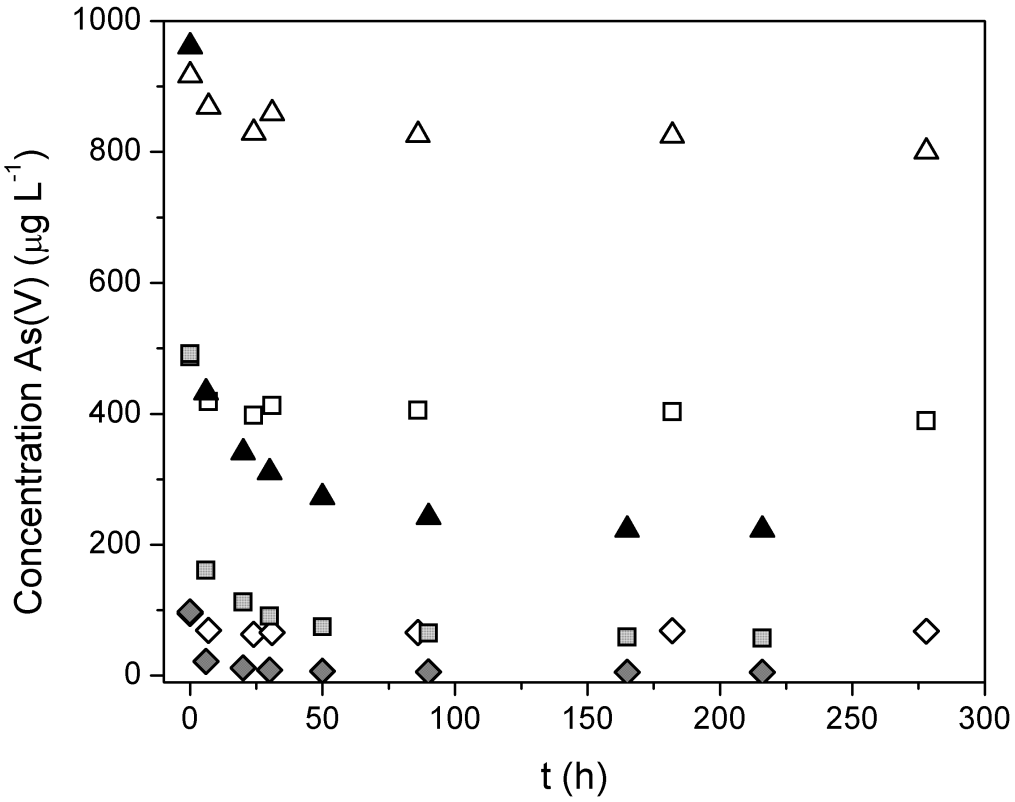

FIGURE 4. Kinetic decay curves for the removal of As(V) by BP-H_2O (open symbols) and BP-H_2O-Fe (filled symbols) at different initial concentrations: 100 μg/L (diamonds), 500 μg/L (squares) and 1000 μg/L (triangles).

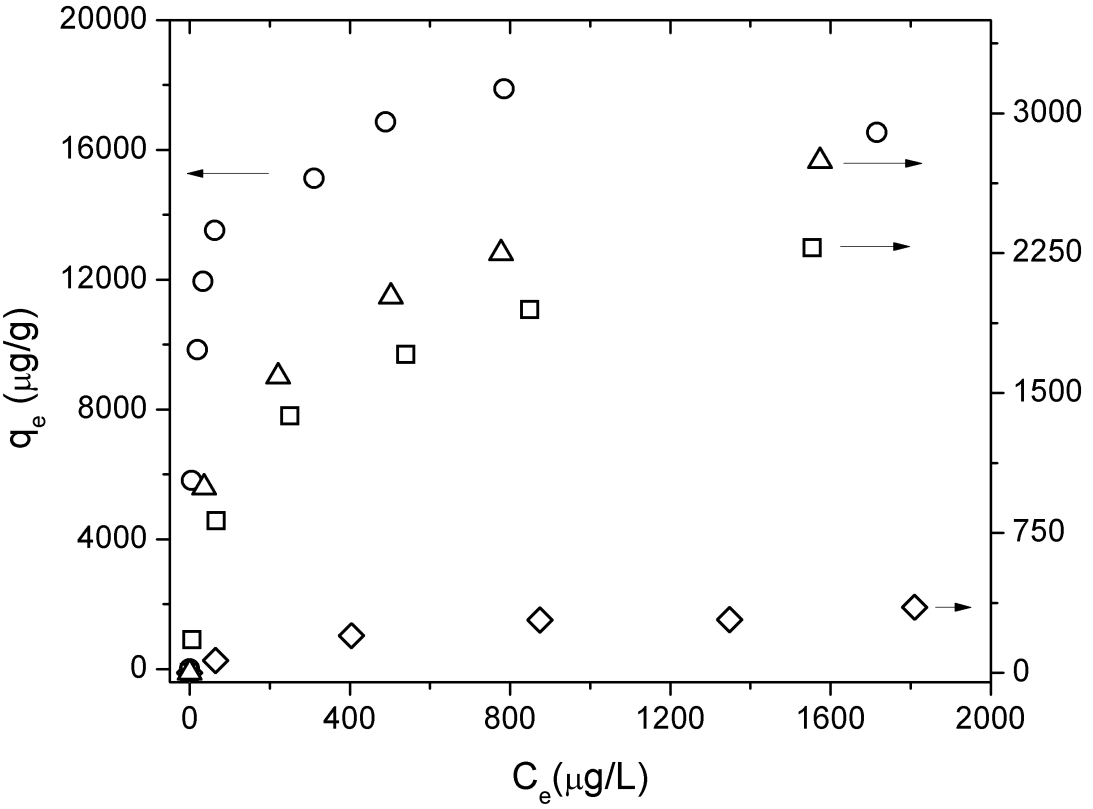

FIGURE 5. Experimental adsorption isotherms of arsenate onto BP-H_2O (diamonds), BP-H_2O-Fe (squares), BP-H_2O-H_2O_2-Fe (triangles) and BP-H_2O-MnO_2-Fe (circles).

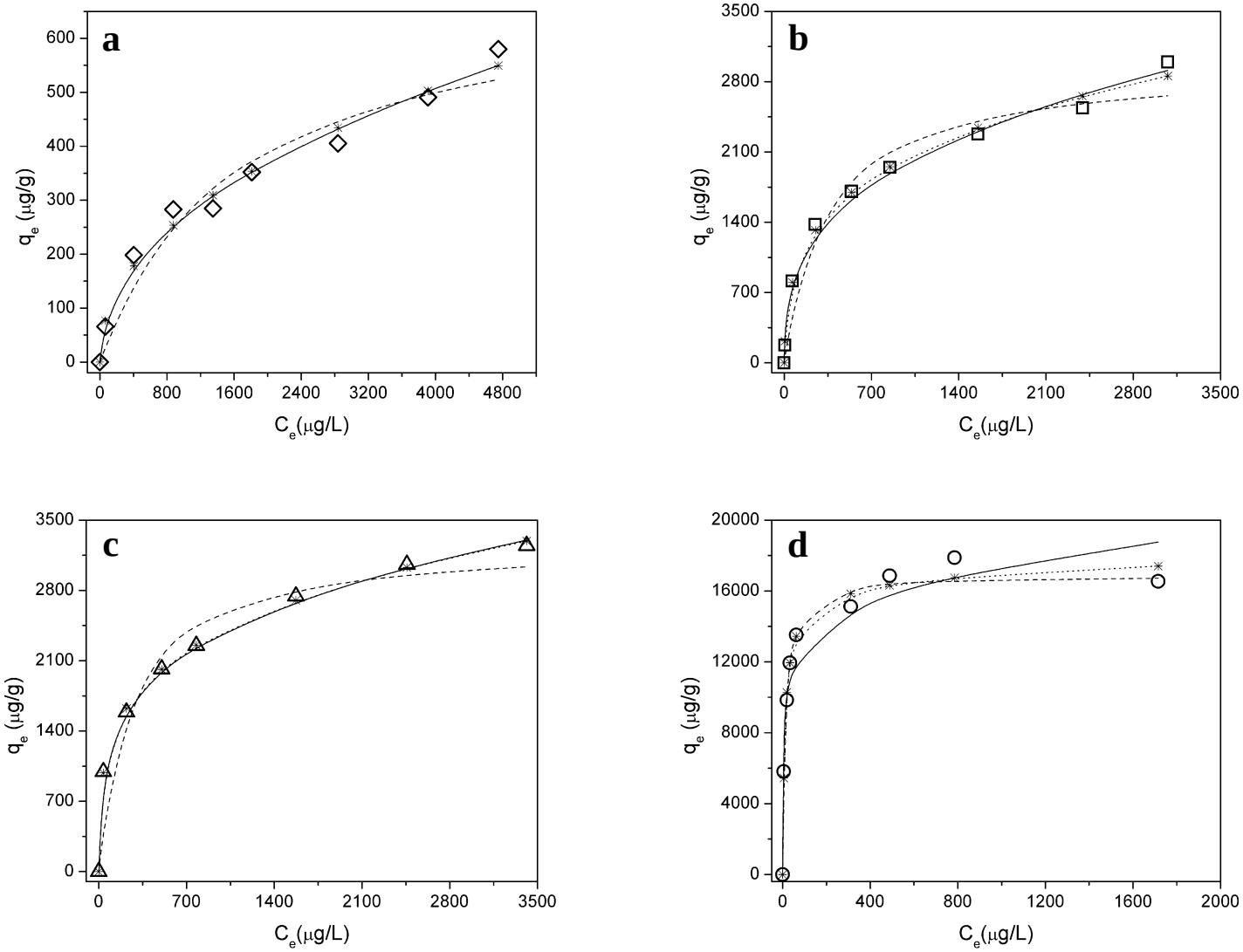

FIGURE 6. Adsorption isotherm for (a) BP-H_2O, (b) BP-H_2O-Fe, (c) BP-H_2O-H_2O_2-Fe and (d) BP-H_2O-MnO_2-Fe. The lines correspond to Langmuir (discontinuous), Freundlich (continuous) and Redlich-Peterson (dotted with starts) models.

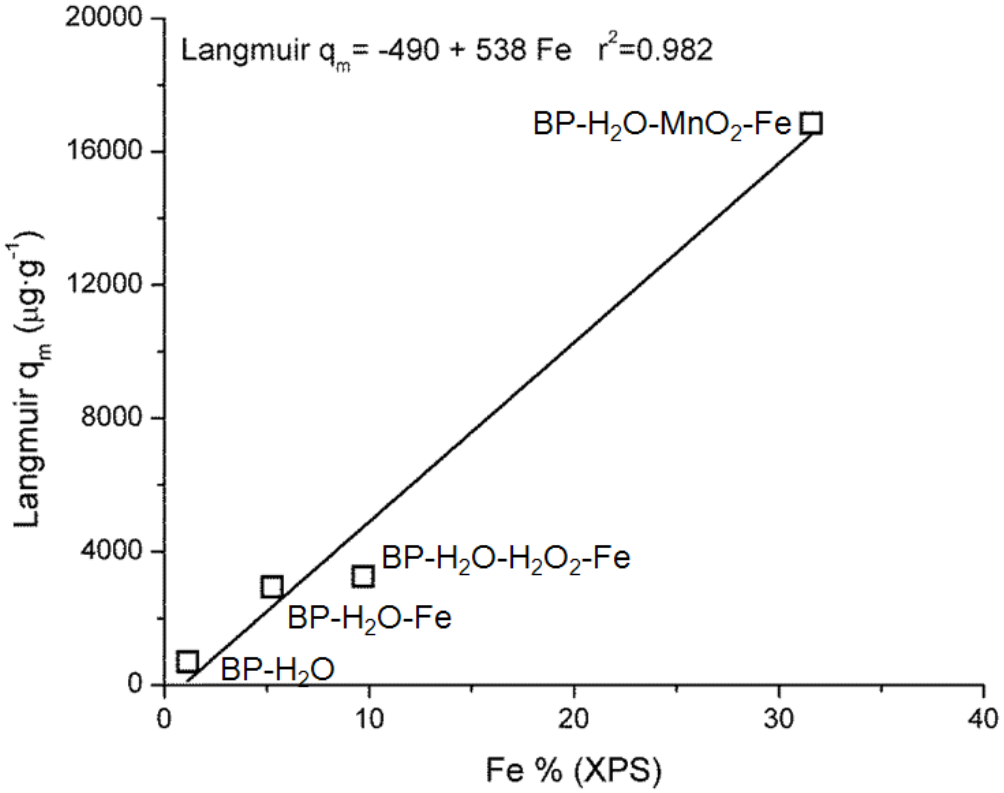

FIGURE 7. Relation between q_m and the corresponding iron content (Fe % from XPS analysis).